https://doi.org/10.1007/s41230-018-8018-1

Microstructure and mechanical properties of AZ91-Ca magnesium alloy cast by different processes

***Xiao-yang Chen, Yang Zhang, Ya-lin Lu, and Xiao-ping Li**

Key lab of advanced Materials Design and Additive Manufacturing of Jiangsu Province, Jiangsu University of Technology, Changzhou 213001, China

Abstract: The microstructure and mechanical properties of magnesium (Mg) alloys are significantly influenced by the casting process. In this paper, a comparative study on microstructure and mechanical properties at ambient and elevated temperatures of AZ91-2wt.% Ca (AZX912) Mg alloy samples prepared by gravity casting (GC), squeeze casting (SC) and rheo-squeeze casting (RSC), respectively, was carried out. The results show that α-Mg grains in SC and RSC samples are significantly refined compared to the GC sample. The average secondary dendritic arm spacing of AZX912 alloy samples decreases in the order of GC, SC and RSC. As testing temperature increases from 25 °C to 200 °C, strength of AZX912 alloy samples is reduced, while their elongation is increased continuously. Compared to GC and SC processes, RSC process can improve the mechanical properties of AZX912 alloy at both ambient and elevated temperatures. The enhancement of mechanical properties of RSC sample over GC and SC samples mainly results from grain refinement in the as-cast microstructure of AZX912 alloy.

Key words: magnesium alloys; casting process; microstructure; mechanical properties

CLC numbers: TG146.22 **Document code:** A **Article ID:** 1672-6421(2018)04-263-07

The application of light weight Mg alloys in the automobile industry is expected to achieve weight reduction and therefore reduce greenhouse gas emissions[1-3]. Since AZ91 alloy (Mg-9Al-1Zn, wt.%) exhibits good comprehensive properties among existing commercial cast Mg alloys, including castability, corrosion resistance and mechanical properties at ambient temperature, it is widely used in the areas of automobile, aerospace and electronic industries. Rare earth and alkaline earth elements are often added into AZ91 alloy to further improve its certain properties. For example, the addition of alkaline-earth element Ca into AZ91 alloy improves its ignition proof resistance by the formation of compact oxide film on the melt surface. Moreover, added Ca element can inhibit the formation of metallurgically unstable $Mg_{17}Al_{12}$ phase and promote the formation of Ca-containing phases with high thermal stability, which is able to improve the heat resistance of AZ91 alloy at elevated temperature [4, 5].

***Xiao-yang Chen**

Female, born in 1987, Ph. D, Lecturer.

Research interest: high-performance magnesium alloys and their forming technologies.

E-mail: cxy@jsut.edu.cn

Received: 2018-02-28; Accepted: 2018-05-14

Previous studies mainly focused on the influence of different Ca contents on phase constituents, microstructure and certain properties of AZ91-Ca alloys [6, 7], while the comparative study on the effect of casting process on microstructure and mechanical properties was scarcely found. Since Mg alloys are generally used in the as-cast state, the mechanical properties of Mg alloys cast by different processes usually differ from each other due to different microstructure characteristics [8]. Caceres et al. [9] compared the microstructure and mechanical properties of AZ91 alloy prepared by sand casting and die casting and the difference in mechanical properties was attributed to different degrees of contribution from work hardening, dispersion strengthening, solid solution strengthening and grain boundary strengthening. Zhu et al. [10] studied the creep behavior of a Mg-Al-Ca alloy (MRI153) prepared by ingot casting, squeeze casting and die casting, respectively. It was found that the creep behavior of MRI153 alloy was influenced by the size of α-Mg grains and relative volume fraction of eutectic particles in the as-cast microstructure, which were both determined by the casting process.

Compared with gravity casting (GC), the mold filling and solidification of squeeze casting (SC) is achieved under applied pressure. Therefore, the comprehensive mechanical properties of components prepared by SC

are significantly improved and the casting soundness is ensured [11, 12]. Rheo-squeeze casting (RSC) is a newly developed semi-solid rheo-forming process, which takes advantage of both rheo-forming and SC. In RSC process, the melt is prepared to be semi-solid slurry containing a certain amount of solid phase, and the prepared semi-solid slurry is then formed in SC process. Wu et al. [13, 14] reported that RSC process was proved to be effective in improving the mechanical properties of a series of Al alloys and a novel Mg-RE-Zn-Y alloy.

In the present work, the microstructure and mechanical properties at ambient and elevated temperatures of AZ91-2wt.%Ca (AZX912) alloy cast by different processes (including GC, SC and RSC) were investigated. The relationship between microstructure characteristics and mechanical properties of AZX912 alloy cast by different processes is discussed.

1 Experimental procedure

In this study, AZX912 alloy was prepared with commercial AZ91D alloy ingots and pure metal Ca (99.9 wt.%). Inductively coupled plasma analyzer (ICP) was used to determine the chemical composition of AZX912 alloy and the real chemical composition was calculated to be Mg-8.21Al-0.53Zn-0.20Mn-1.76Ca (wt.%). Under the protection atmosphere [a mixed gas of SF6 (1vol.%) and CO_2 (99vol.%)], the pre-weighed AZ91D ingot was heated and melted. When the temperature of AZ91D melt reached 700 °C, pure metal Ca was added. Later, the melt was stirred for 3 min to ensure the dissolution and homogeneous distribution of Ca. Then the melt was heated to 700 °C again for the further preparation of semi-solid slurry.

The details of RSC process of AZX912 alloy were demonstrated in Ref. [15]. For the RSC sample used in this study, the gas flow in preparation of semi-solid slurry of AZX912 alloy was set as 6 L·min^{-1}, the pouring temperature of semi-solid slurry was set as 596 °C and the applied pressure used for RSC process was set as 120 MPa. In SC process, the applied pressure was also set as 120 MPa and the pouring temperature was set as 700 °C. In GC process, the pouring temperature was also set as 700 °C while no pressure was applied during casting. The size of cast samples was Φ55×80 mm.

Specimens for microstructure characterization were cut from the cast samples and prepared with standard metallographic procedures. Optical microscope (OM, ZEISS, Axio observer A1) and scanning electron microscope (SEM, Quanta FEG 250) were used for microstructure characterization. Quantitative image analysis software (Imagepro-plus 6.0) was used for metallographic analysis. Therefore, the average secondary dendritic arm spacing of AZX912 alloy samples cast by different processes is calculated by quantitative metallographical analysis. The phases in the microstructure of alloys were identified by X-ray diffraction (XRD, D/max 2550VL/PC) with Ni-filtered Cu-Kα radiation. Rectangular tensile specimens with a guage length of 10 mm were cut from the cast samples. Zwick/Roell-20 kN material test machine was used for ambient temperature (25 °C) tensile testing according to ISO6892-1:2009 and SHIMADZU AG-100KNA tensile machine was used for elevated temperature tensile testing according to ISO6892-2: 2011. The cross-head speed for both ambient and elevated temperature tensile testings was 1 mm·min^{-1}.

2 Results

Figure 1 shows analysis results of XRD patterns of AZX912 alloy samples cast by different processes. According to XRD results, all three samples consist of α-Mg, β-$Mg_{17}Al_{12}$ and Al_2Ca phases. XRD results confirm that change of casting process shows little influence on phase constituents of AZX912 samples.

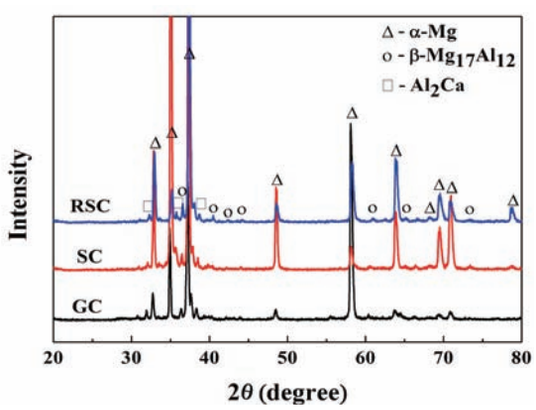

Fig. 1: XRD patterns and analysis results of AZX912 alloy samples cast by different processes

Figure 2 shows optical microstructures of AZX912 alloy samples cast by different processes. As shown in Fig. 2, change of casting process significantly influences the microstructure of AZX912 alloy. In these three samples, α-Mg phase shows significant difference, including size and morphology. In GC sample (Fig. 2a), α-Mg phase is coarsely dendritic. Compared with GC sample, dendritic α-Mg phase in SC sample (Fig. 2b) is obviously refined. Unlike GC or SC samples, the microstructure of RSC sample exhibits typically semi-solid characteristic. In RSC sample (Fig. 2c), α-Mg phase includes two parts, i.e. large non-dendritic particles and well-refined dendrites. The large non-dendritic particles are primary α-Mg phase which nucleated and grew during the gas bubbling for semi-solid slurry preparation and the well-refined dendrites formed in the residual melt in the subsequent SC of prepared AZX912 semi-solid slurry. The average secondary dendritic arm spacing is usually used to represent the grain refinement of dendritic grains. In this study, both GC and SC samples exhibit completely dendritic microstructure, and the dendritic microstructure is also the majority of RSC sample. According to the results in Fig. 2d, the average secondary dendritic arm spacing of AZX912 alloy samples decreases in the order of GC, SC and RSC.

Figure 3 shows SEM images of AZX912 alloy samples cast by different processes. The SEM images show that change of casting process also has significant effect on the size and morphology of second phase particles in AZX912 alloy. As

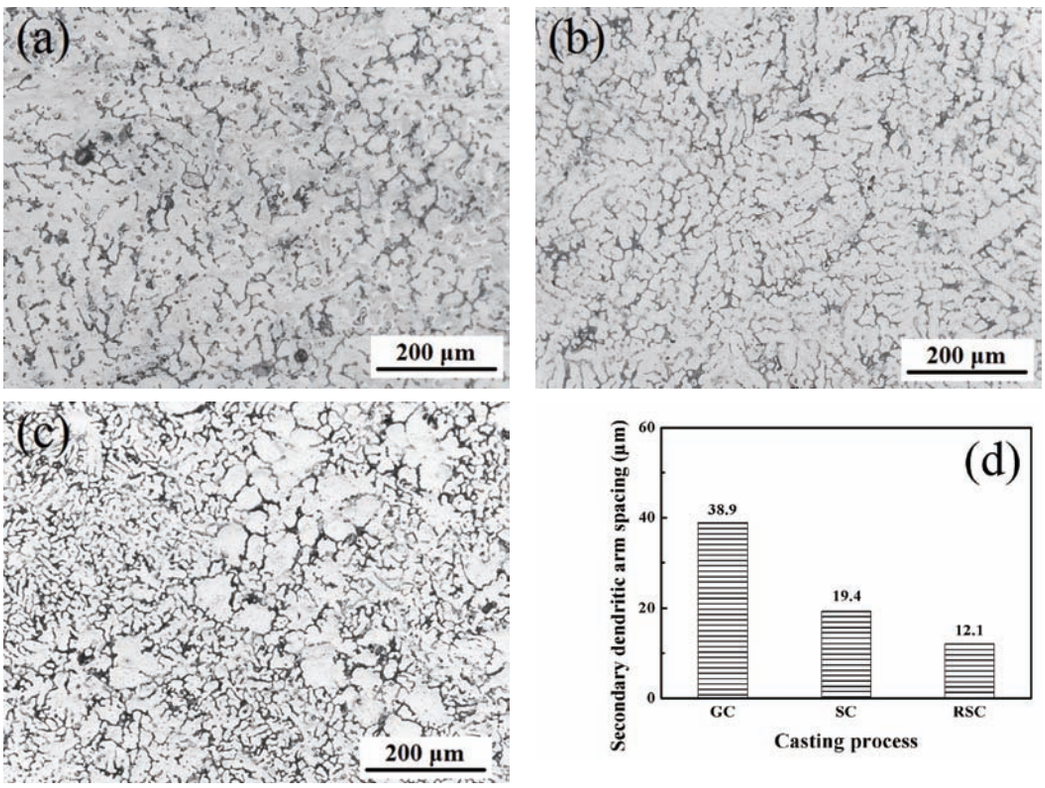

Fig. 2: Optical microstructure and average secondary dendritic arm spacing of AZX912 alloy samples cast by different processes: (a) optical microstructure of GC; (b) optical microstructure of SC; (c) optical microstructure of RSC and (d) average secondary dendritic arm spacing

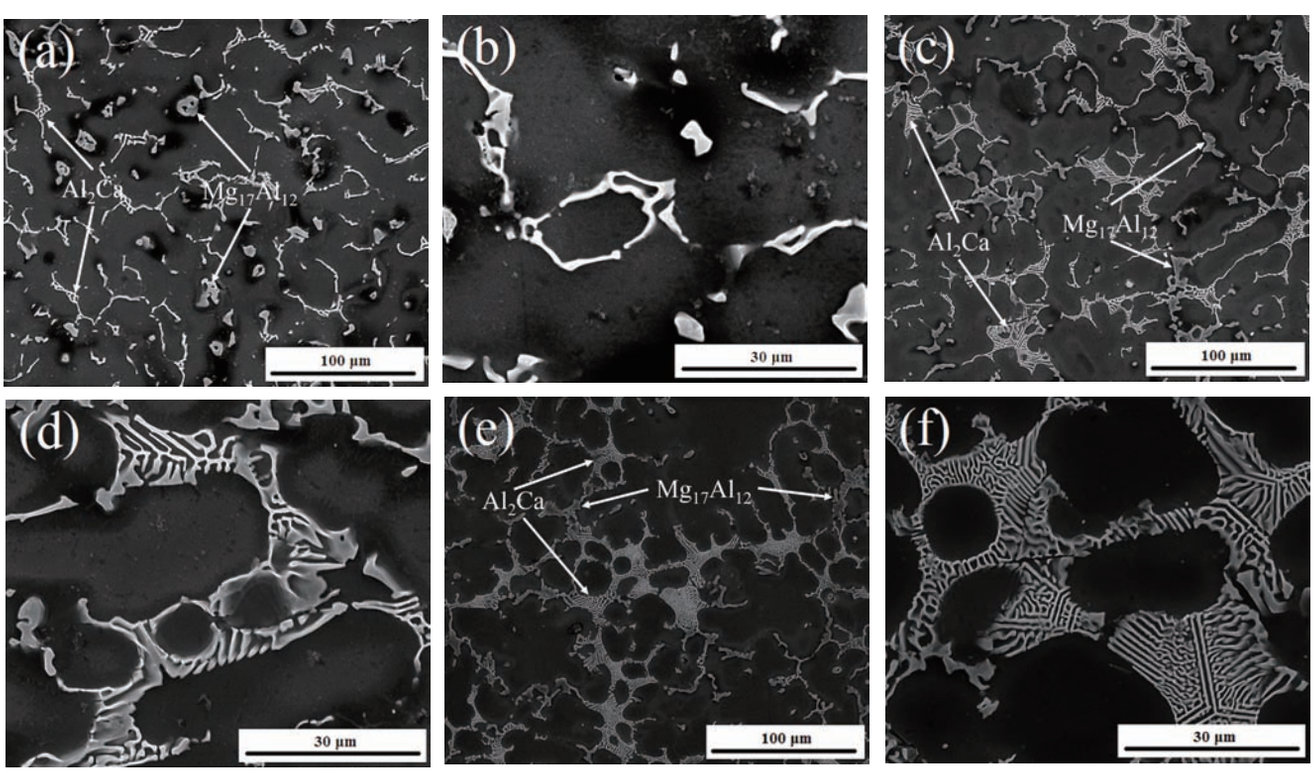

Fig. 3: SEM images of AZX912 alloy samples cast by different processes: (a, b) GC; (c, d) SC and (e, f) RSC

shown in Fig. 3, Al_2Ca phase is the main second phase in AZX912 alloy. In GC sample (Fig. 3a), second phase distributes evenly among the coarse dendritic arms and their size is relatively large. In SC sample (Fig. 3b), second phase still distributes among the dendritic arms, but the size is refined. Al_2Ca phase transfers from single layer to multi layers. The thickness of each layer becomes thin and the gap between adjacent layers reduces. However, in RSC sample (Fig. 3c),

the distribution of second phase is not uniform. Second phase aggregates in the unsolidified residual melt and Al_2Ca phase shows connected network structure. Due to the low pouring temperature in RSC process, Al_2Ca phase is further refined, which promotes the dendritic growth of Al_2Ca phase.

It is also observed from SEM images that the relative content of second phases in AZX912 alloy samples varies with the change of casting process. Figure 4 shows the quantitative data of the volume fraction of second phases in AZX912 alloy samples cast by different processes. It is seen from Fig. 4 that the content of second phases in GC sample is only 9.8vol. %. The content of second phases increases to 13.0 vol.% in SC sample and further increases to 15.3vol. % in RSC sample.

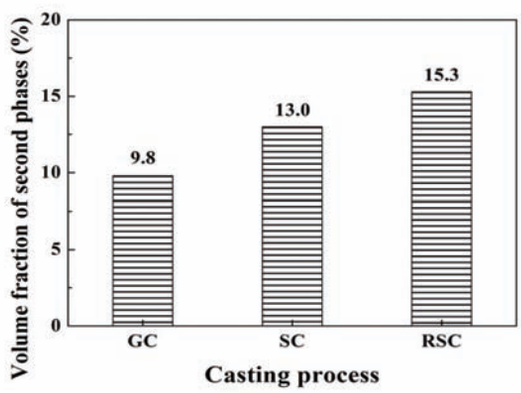

Fig. 4: Effect of casting process on relative content of second phases in AZX912 alloy samples

Figure 5 shows the effect of casting process on mechanical properties of AZX912 alloy samples tested at different temperatures. As shown in Fig. 5(a), GC sample tested at ambient temperature (~25 °C) shows the worst mechanical properties. Among three samples, RSC sample possesses the best mechanical properties at ambient temperature. YS, UTS and E_f of RSC sample reach 110.2 MPa, 177.9 MPa and 3.3%, respectively, which are 48.3%, 39.1% and 106.2% higher than the corresponding values of GC sample and 27.1%, 22.8% and 83.3% higher than the corresponding values of SC sample, respectively. As can be seen from Fig. 5(b-d), in the testing temperature range of 100–200 °C, RSC sample also exhibits the best mechanical properties and GC sample is the worst, which is similar to the law when tested at ambient temperature. Even at 150 °C, RSC sample still possesses relatively high strength and its YS, UTS and E_f are 85.2 MPa, 142.3 MPa and 5.6%, respectively. Compared with its mechanical properties at ambient temperature, the decrease in strength is only about 20%. Meanwhile, by comparison with GC and SC samples, it is found that, both YS and UTS of RSC sample at 150 °C are higher than those of GC sample and close to those of SC sample tested at ambient temperature. When testing temperature increases to 200 °C, the drop of strength accelerates while the ductility improves obviously in all three samples. At testing temperature of 200 °C, YS, UTS and E_f of RSC sample are 68.6 MPa, 116.8 MPa and 12.2%, respectively. Compared with its mechanical properties at ambient temperature, the decrease in strength is nearly 40% while the increase in ductility is more than 270%. These comparative results prove that RSC process can significantly

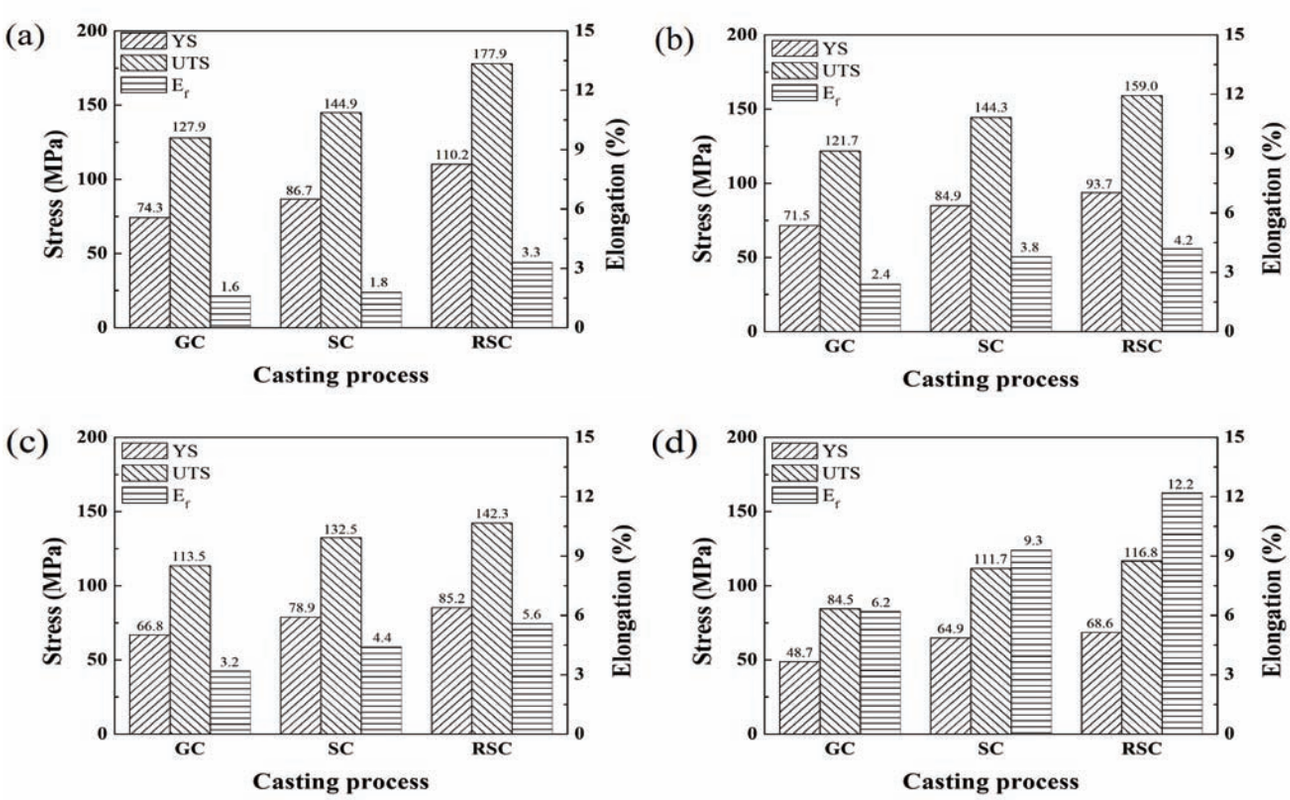

Fig. 5: Effect of casting process on mechanical properties of AZX912 alloy samples tested at different temperatures: (a) 25 °C; (b) 100 °C; (c) 150 °C and (d) 200 °C

improve the mechanical properties of AZX912 alloy at both ambient and elevated temperatures compared with conventional GC and SC process.

In order to clarify the fracture behavior of AZX912 alloy samples cast by different processes, the fracture surface of tensile samples tested at 100 °C and 200 °C, respectively, is observed by SEM. Figure 6 shows fracture morphology of tensile sample tested at 100 °C. It can be seen that the fracture surface of three AZX912 samples exhibits the typical characteristic of brittle fracture mode. The difference in grain size is also presented in the fracture surface of three samples. Resulting from the fine grain size, the fracture surfaces of SC and RSC samples are much smoother than that of GC sample. As shown in Fig. 6(a,b), crack of matrix is observed in high magnification image of GC sample, indicating its poor ductility. The brittle fracture morphology of AZX912 samples tensile tested at 100 °C is in accordance with the relatively low elongation shown in Fig. 5(b).

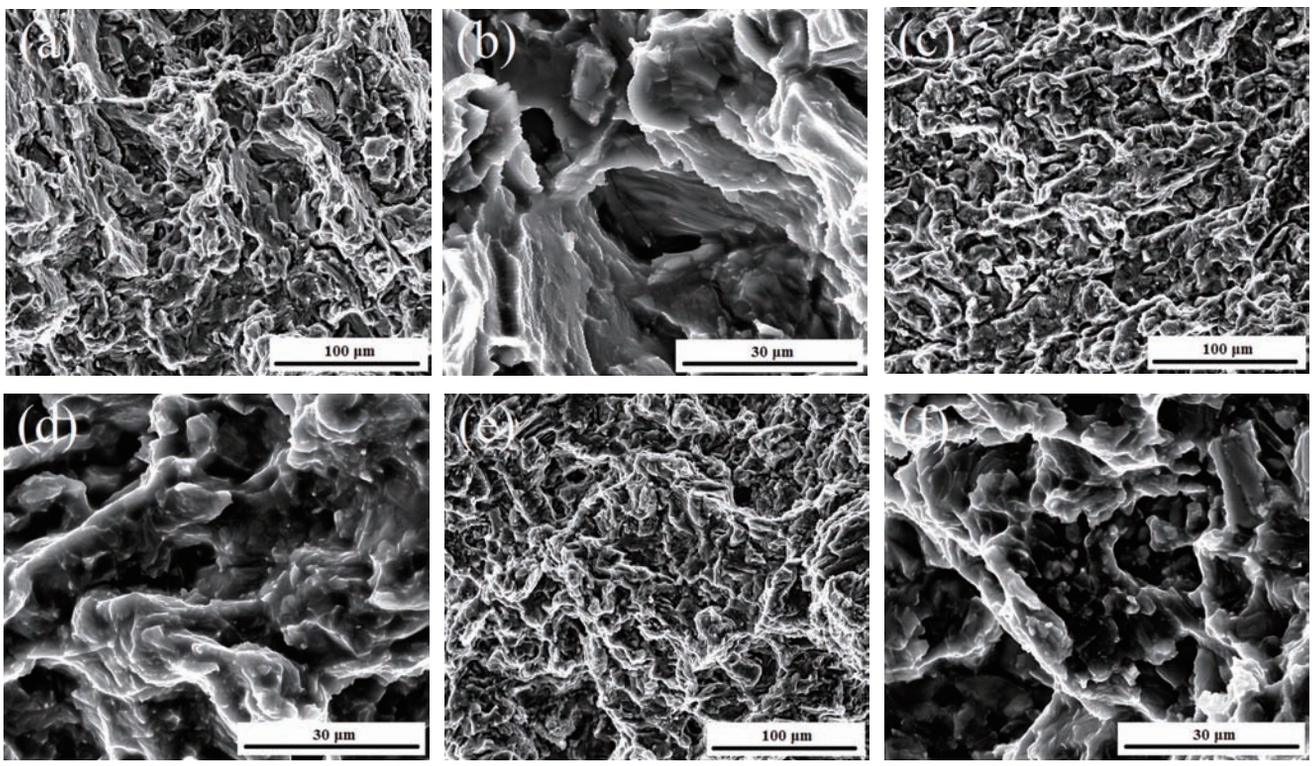

Fig. 6: Effect of casting process on the fracture morphology of AZX912 alloy samples tensile tested at 100 °C: (a, b) SC; (c, d) SC and (e, f) RSC

Figure 7 shows fracture morphology of AZX912 alloy samples tensile tested at 200 °C. As shown in Fig. 7(a, b), fracture surface of GC sample still exhibits the characteristic of brittle fracture mode. However, as shown in Fig. 7(c-f), some dimples appear in the fracture surface of SC and RSC samples, which indicates that their fracture mode partly changes from brittle to ductile. The change of fracture mode is also proved by the obvious improvement of elongation when testing temperature increases from 100 to 200 °C.

3 Discussion

Generally, the enhancement of cooling rate during solidification can promote grain refinement for as-cast microstructure. In conventional GC process, superheated melt is poured into the mold and then solidified under atmosphere. In this study, the pouring temperature is 700 °C and the liquidus of AZX912 alloy is about 600 °C. Therefore, the degree of superheat is about 100 °C. During the solidification of GC, the superheat and latent heat of the melt are transferred from the melt to the mold. However, due to the existence of solidification shrinkage, after the pouring of the melt, an air gap forms immediately between the internal surface of the mold and the outside surface of solidified shell in GC process. The presence of air gap hinders the heat transfer and reduces the cooling rate significantly. As a result, cooling rate of GC is the lowest in all three casting processes used in this study. In SC process, pressure is applied to the melt within several seconds after the pouring of superheated melt into the mold. Solidification under applied pressure can eliminate the air gap and keep the internal surface of the mold and the outside surface of solidified shell contact closely. The close contact interface helps the heat transfer from melt to mold [16]. Therefore, the cooling rate in SC is much higher than that in GC. Meanwhile, based on Clausius-Clapeyron equation:

$$\frac{\Delta T_f}{\Delta P} = \frac{T_f (V_l - V_s)}{\Delta H_f} \quad (1)$$

where T_f is the equilibrium freezing temperature, V_l and V_s are the specific volumes of the liquid and solid, respectively, and

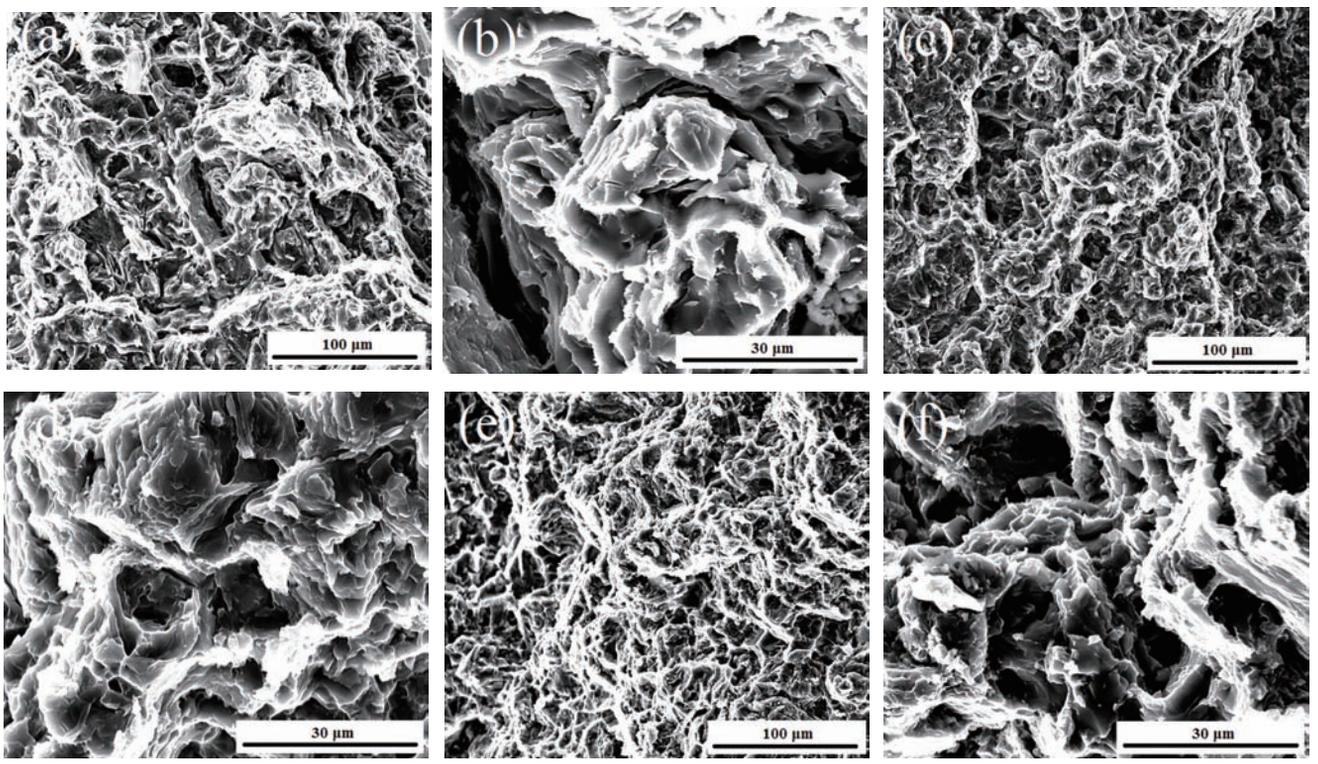

Fig. 7: Effect of casting process on fracture morphology of AZX912 alloy samples tensile tested at 200 °C: (a, b) SC; (c, d) SC and (e, f) RSC.

ΔH_f is the latent heat of fusion, the influence of pressure on the freezing point may be roughly estimated as follows:

$$P = P_0 \exp(\frac{-\Delta H_f}{RT_f}) \quad (2)$$

where P_0, ΔH_f and R are constants. According to Eq. (2), as pressure increases, T_f should increase simultaneously. According to solidification theory, increase of T_f can induce a high undercooling and nucleation rate. Unlike GC or SC, the solidification of RSC is discontinuous and it can be roughly divided into two steps: first is the nucleation and growth of primary α-Mg phase in semi-solid slurry and second is subsequent SC of semi-solid slurry. Accordingly, refinement of RSC also consists of two parts: first is the refinement of primary phase and second is the rapid cooling in following SC process. After gas bubbling, both temperature and concentration distribution are relatively homogeneous in residual melt. Compared with GC and SC, melt poured into mold in RSC is prepared into semi-solid slurry, rather than superheated melt. Semi-solid slurry is a mixture of primary solid particles and undercooled melt. During SC of semi-solid slurry, there is no superheat to be released. Therefore, compared with SC, the cooling rate during RSC is further improved, which leads to the formation of well-refined dendrites in the residual melt. The microstructure of RSC sample consists of coarse non-dendritic α-Mg particles and fine dendrites, which is a typical bimodal grain distribution. It is reported that the bimodal structure can coordinate the deformation among grains and improve the strength and ductility of alloys simultaneously [17]. During the deformation, the coarse α-Mg particles act as the soft and ductile part, which is able to inhibit the extension of localized deformation band and initiate more deformation bands. As a result, the ductility of RSC sample is improved. In addition, the hard and fine dendrites around the coarse α-Mg particles can restrict the dislocation multiplication via inhibiting the dislocation movement through grain boundaries. Therefore, the strength of RSC sample is also improved.

Meanwhile, second phase in AZX912 samples is refined significantly with enhancement of the cooling rate. The increase of cooling rate and application of pressure also lead to increase of amount of second phase. High cooling rate and applied pressure promote the deviation of phase diagram from the equilibrium condition. According to the calculation concerning influence of pressure on phase diagram of Mg-Al binary alloy[18], application of pressure leads to the increase of the temperature of liquidus and solidus curves. In addition, the eutectic point is also moved to the Mg-rich region. Increase of the cooling rate has a similar effect. Movement of eutectic point to Mg-rich region leads to increase of content of second phases. Unlike the relatively even distribution in GC or SC sample, second phases in RSC sample aggregate in the solidified residual melt and form connected-network structure [19]. The preparation of semi-solid slurry in RSC process exacerbates the enrichment of alloying elements in residual melt, which leads to the growth of network-like Al_2Ca phase. Since Al_2Ca phase is brittle at ambient temperature, it is easily broken during deformation and becomes a crack initiation. The existence of Al_2Ca phase has a negative effect on comprehensive mechanical properties of AZX912 alloy. However, when RSC sample was tensile tested at ambient temperature, it still exhibits the best mechanical properties.

Grain size is also important for elevated temperature mechanical properties of AZX912 alloy. According to Hall-Petch rule, grain refinement is an effective strengthening mechanism at ambient temperature, which is also confirmed in this study. However, with the increase of testing temperature, the classic Hall-Petch equation is no longer satisfied. At elevated temperature, the atoms at the grain boundary regions have high energy and their activity, therefore, is enhanced. Since there are more vacancies and dislocations at the grain boundary than in the intercrystalline, grain boundaries become weak during deformation at elevated temperature, and intergranular plastic deformation is prone to take place [20]. However, in this study, even at 200 °C, RSC sample still exhibits the best mechanical properties among the three samples, since RSC sample possesses the finest grain size. These results indicate that, for AZX912 components whose typical application is lower than 200 °C, RSC process is effective in improving its mechanical properties at both ambient and elevated temperatures.

4 Conclusions

(1) As-cast microstructure of AZX912 alloy samples is significantly influenced by the casting process. In GC sample, α-Mg phase is coarsely dendritic. In SC sample, dendritic α-Mg phase is refined obviously. In RSC sample, α-Mg phase includes large non-dendritic particles and well-refined dendrites. Change of casting process also has great effects on size, morphology and distribution of second phases in AZX912 alloy.

(2) When tensile tested at both ambient and elevated temperatures, RSC sample exhibits the best mechanical properties while GC sample exhibits the poorest mechanical properties. As testing temperature increases, YS and UTS of three samples decrease and E_f increases. All three samples show the brittle fracture mode at 100 °C, while the fracture mode of SC and RSC samples partly changes from brittle to ductile when tested at 200 °C.

(3) The mechanical properties of AZX912 alloy samples are determined by the microstructure. The enhancement of mechanical properties of RSC sample over GC and SC samples mainly results from grain refinement in as-cast microstructure.

References

[1] Kabirian F, Mahmudi R. Effects of Rare Earth Element Additions on the Impression Creep Behavior of AZ91 Magnesium Alloy. Metallurgical & Materials Transactions A, 2009, 40: 2190–2201.

[1] Wu Mengwu, Hua Lin, Xiong Shoumei. Modeling studies on divorced eutectic formation of high pressure die cast magnesium alloy. China Foundry, 2018, 15: 58–65.

[2] Zhang Guang, Qiu Keqiang, Xiang Qingchun, et al. Creep resistance of as-cast Mg-5Al-5Ca-2Sn alloy. China Foundry, 2017, 14: 265–271.

[3] Wang Jing, Fang Xiaogang, Wu Shusen, et al. Effects of heat treatment on microstructure evolution and mechanical properties of Mg-6Zn-1.4Y-0.6Zr alloy. China Foundry, 2017, 14: 199–204.

[4] Amberger D, Eisenlohr P, Göken M. Microstructural evolution during creep of Ca-containing AZ91. Materials Science & Engineering A, 2009, 510: 398–402.

[5] Amberger D, Eisenlohr P, Göken M. On the importance of a connected hard-phase skeleton for the creep resistance of Mg alloys. Acta Materialia, 2012, 60: 2277–2289.

[6] Wu Guohua, Fan Yu, Gao Hongtao, et al. The effect of Ca and rare earth elements on the microstructure, mechanical properties and corrosion behavior of AZ91D. Materials Science & Engineering A, 2005, 408: 255–263.

[7] Li Perijie, Tang Bin, Kandalova E G. Microstructure and properties of AZ91D alloy with Ca additions. Materials Letters, 2005, 59: 671–675.

[8] StJohn D H , Ma Q, Easton M A , et al. Grain refinement of magnesium alloys. Metallurgical & Materials Transactions A, 2005, 36: 1669–1679.

[9] Caceres C H, Davidson C J, Griffiths J R, et al. Effects of solidification rate and ageing on the microstructure and mechanical properties of AZ91 alloy. Materials Science & Engineering A, 2002, 325: 344–355.

[10] Zhu S M, Mordike B L, Nie J F. Creep properties of a Mg-Al-Ca alloy produced by different casting technologies. Materials Science & Engineering A, 2008, 483: 583–586.

[11] Ghomashchi M R, Vikhrov A. Squeeze casting: an overview. Journal of Materials Processing Technology, 2000, 101: 1–9.

[12] Goh C S, Soh K S, Oon P H, et al. Effect of squeeze casting parameters on the mechanical properties of AZ91-Ca Mg alloys. Materials & Design, 2010, 31: S50–S53.

[13] Lü Shulin, Wu Shusen, Dai Wei, et al. The indirect ultrasonic vibration process for rheo-squeeze casting of A356 aluminum alloy. Journal of Materials Processing Technology, 2012, 212: 1281–1287.

[14] Fang Xiaogang, Lü Shulin, Zhao Li, et al. Microstructure and mechanical properties of a novel Mg-RE-Zn-Y alloy fabricated by rheo-squeeze casting. Materials & Design, 2016, 94: 353–359.

[15] Zhang Yang, Wu Guohua, Liu Wencai, et al. Preparation and rheo-squeeze casting of semi-solid AZ91-2wt.% Ca magnesium alloy by gas bubbling process. Journal of Materials Research, 2015, 30: 825–832

[16] Masoumi Mohsen, Hu Henry. Influence of applied pressure on microstructure and tensile properties of squeeze cast magnesium Mg-Al-Ca alloy. Materials Science & Engineering A, 2011, 528: 3589–3593.

[17] He J H, Jin L, Wang F H, et al. Mechanical properties of Mg-8Gd-3Y-0.5Zr alloy with bimodal grain size distributions. Journal of Magnesium & Alloys, 2017, 5: 423–429.

[18] Hu H. Squeeze casting of magnesium alloys and their composites. Journal of Materials Science, 1998, 33: 1579–1589.

[19] Kleiner S, Ogris E, Beffort O, et al. Semi Solid Metal Processing of Aluminum Alloy A356 and Magnesium Alloy AZ91: Comparison Based on Metallurgical Consideration. Advanced Engineering Materials, 2003, 5: 653–658.

[20] Li Yanlei, Wu Guohua, Chen Antao, et al. Effects of Gd and Zr additions on the microstructures and high-temperature mechanical behavior of Mg-Gd-Y-Zr magnesium alloys in the product form of a large structural casting. Journal of Materials Research, 2015, 30: 3461–3473.

This work was financially supported by the National Natural Science Foundation of China (No. 51601076) and the Natural Science Fund for Colleges and Universities in Jiangsu Province (No. 16KJB430013, 17KJA430005).